Experimental Extraction of Winding Resistance in Litz-Wire Transformers—Influence of Winding Mutual Resistance

Korawich Niyomsatian, *Student Member, IEEE*, Johan J. C. Gyselinck, *Member, IEEE*, and Ruth V. Sabariego

***Abstract*—The extraction of winding resistance from impedance measurements needs a compensation of undesirable effects, e.g., core loss and distributed winding capacitance. This paper rigorously shows that the core loss (or core-loss resistance) measured with the two-winding method always includes the effect of the winding mutual resistance. At high frequencies, this effect becomes more prominent and can cause an overestimation of the measured core-loss resistance. As a result, the compensated winding resistances can be significantly underestimated. To mitigate this effect, this paper proposes to measure the core-loss resistance on an auxiliary 1:1 transformer with single-turn windings. Consequently, it is scaled to obtain the actual core loss. The proposed analysis and method is applicable to multiwinding systems. For validation, this paper considers a gapped transformer with litz-wire winding for high-frequency operations. The experimental results are validated against the results from its three-dimensional finite-element (FE) model. The litz-wire winding is considered in the FE model by means of a homogenization approach. With the method proposed in this paper, the experimentally extracted winding resistances become more accurate and are in good agreement with the FE results.**

***Index Terms*—Eddy current, finite-element (FE) methods, HF transformers, resistance measurement, transformer windings.**

I. Introduction

Apart from core loss, winding loss is an integral part of the losses of magnetic devices and it has become more significant in modern-day high-frequency applications. Aiming for a high-efficiency magnetic device, the experimental verification of winding loss from winding resistance is an essential procedure after the design process since a prototype always includes nonideal factors, e.g., tolerance of litz-wire construction and core shape, which are difficult to be considered exhaustively during the modeling and design processes. For a device with n_{w} windings, its winding loss is governed by frequency-dependent $n_{\mathrm{w}}\,(n_{\mathrm{w}}-1)/2$ winding mutual resistances in addition to conventional n_{w} winding self-resistances [1]. Mutual resistance between any two windings represents the additional power loss in all the windings when the currents in both windings are nonzero. This winding mutual resistance is normally negligible at low frequencies, but it becomes significant at high frequencies particularly when windings are wound close to one another to achieve tight coupling (proximity effect).

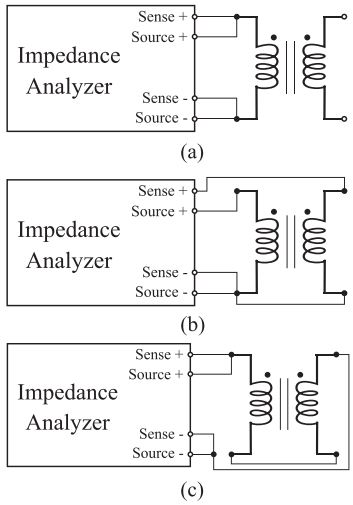

Fig. 1. Configurations to measure winding resistances of a two-winding device with an impedance analyzer [3]. The DUT is excited through the source terminals of an impedance analyzer with the adjustable voltage source and with the known current, whereas the voltage across the winding can be measured with the sense probes. (a) Self-resistance measurement. (b) Small-signal core-resistance measurement (Conventional two-winding method). (c) Leakage connection.

Despite being a simple and linear property when a core is in its linear region under small excitation, determining the winding resistance from impedance measurements can be difficult due to the excited core loss. The self-resistance obtained from a measurement of resistance at the terminal of a winding [see Fig. 1(a)] includes the small-signal core-loss resistance in addition to the desired winding self-resistance [2]. Despite using low-loss ferrite cores, this core-loss resistance can yield more than 10%–20% error above a few hundred kilohertz [3]. Notably, the winding resistance of a device under test (DUT) should not be measured without its magnetic core because the presence of the core and airgap can greatly affect both the field distribution in the winding region and the winding resistance. Therefore,

Manuscript received July 30, 2018; revised September 13, 2018; accepted October 8, 2018. Date of publication October 15, 2018; date of current version May 2, 2019. This paper is supported by the EU funded Marie Curie ITN ADvanced Electric Powertrain Technology (ADEPT) project (grant number 607361). Recommended for publication by Associate Editor W. Huang. *(Corresponding author: Korawich Niyomsatian.)*

K. Niyomsatian and R. V. Sabariego are with the Department Electrical Engineering, KU Leuven, 3001 Leuven-Hervelee, Belgium, and also with EnergyVille, 3600 Genk, Belgium (e-mail:

determining the core loss and its compensation are crucial. According to a recent study [3], the predicted core loss based on the complex permeability in a datasheet can significantly differ from the actual one due to different testing conditions. Instead, the measurement of the actual core loss is recommended, which can be done with the two-winding method.

In this paper, all the methods relying on electrical measurements and two windings are considered as the "two-winding method" [4]–[7]. One winding (excitation winding) is used to excite a core with a known current, while the other winding (sensing winding) is kept open and its terminal voltage is measured [see Fig. 1(b)].[1] Thus, the measured core loss excludes the loss from its winding self-resistances. However, it includes the effect of the winding mutual resistance between the two windings because the measured voltage of the sensing winding is affected by the electric field caused by the excitation winding [3], [5]. Therefore, if the core loss for compensation is carelessly measured by directly performing the two-winding method with the windings of the DUT, the obtained core loss can be erroneous. From our observation of a gapped transformer with a set of two tightly coupled litz-wire windings, the effect of the winding mutual resistance can cause the overestimation of the core-loss resistance, and thus the underestimation of the extracted winding resistance. Despite being mentioned in [1] and [3], to the best of our knowledge, the precise relationship between the winding mutual resistance and the measured core loss has not been rigorously formulated in the literature. In [1], winding loss and a winding-resistance matrix are considered without core loss and no circuit relation between them has been clarified.

A direct way to determine the winding resistance is to use a numerical method [8]–[12], particularly when the resistance is small and difficult to measure accurately, e.g., winding mutual resistance [5]. In this work, we have considered the finite-element (FE) method because of high modeling flexibility and accuracy for complex geometries. Furthermore, to model a litz wire, the homogenization method in [8] and [13] has been adopted. As a result, a litz-wire bundle is replaced by a homogeneous conductor enabling the easy integration into an FE model of a magnetic device, avoiding a huge number of unknowns due to fine discretization of many small conductor strands.[2]

The main original contribution of this paper is a rigorous modeling and illustration of the effect of the winding mutual resistance on the core-loss measurement based on the two-winding method and the corresponding extracted winding self-resistance. Additionally, a compensation of small-signal core-loss resistance is exemplified to alleviate the effect of the winding mutual resistance yielding accurate extracted winding resistance.

The paper begins by reviewing the electrical circuit model of magnetically coupled windings and an equivalent circuit of a two-winding device in Section II. As a result, the paper illustrates the effect of the winding mutual resistance on the core loss measured with the two-winding method in Section III. An improved core-loss compensation is proposed in Section IV. The homogenized model of litz wires in FE models is briefly explained in Section V. As a test case and validation, a gapped transformer with tight coupling is selected, and its three-dimensional (3-D) FE model is developed. The numerical and experimental results are presented in Section VI.

II. Electrical Circuit Model of Magnetically Coupled Windings With a Magnetic Core

A. Device With n_{w} Windings

Considering a frequency-domain magnetodynamic[3] problem of a magnetically coupled linear system with n_{w} galvanically isolated windings and a core being in its linear region due to small excitation, at frequency f (angular frequency $\omega = 2\pi f$), the voltage $\underline{V}_i$ in complex rms-amplitude phasor (underlined symbols with $\mathrm{j} = \sqrt{-1}$) across the terminal of the ith winding can be described in terms of an impedance $\underline{Z}_{ij} = \underline{Z}_{ji} = R_{ij} + \mathrm{j}\omega L_{ij}$ with $i, j = 1, \ldots, n_{\mathrm{w}}$ as

$$\underline{V}_i = \sum_{j=1}^{n_{\mathrm{w}}} \underline{Z}_{ij}\underline{I}_j, \quad i = 1, \ldots, n_{\mathrm{w}} \tag{1}$$

where $\underline{I}_j$ is the current entering the jth winding and $\underline{Z}_{ij}$ is the mutual impedance if $i \neq j$, otherwise, self-impedance $\underline{Z}_{ii}$. Herein, the passive sign convention is adopted. The current $\underline{I}_j$ is defined positive when entering the defined positive voltage terminal of a device. This results in positive R_{ii} and reciprocity, i.e., $R_{ij} = R_{ji}$.

When only the jth winding is excited $\left(\underline{I}_j \neq 0\right)$, an electromagnetic field is induced inside the conductors of the ith winding and vice versa ($i \neq j$), leading to the winding impedance $\underline{Z}_{ij}^{\mathrm{w}}$ between the ith and jth windings (proximity effect [6]). In other words, the current distribution in the ith winding is affected by the presence of the currents (and its generated magnetic field) flowing in the jth winding in its proximity, leading to the change in the voltage drop (electric field) along the winding (conductor). In addition, the current $\underline{I}_j$ creates the magnetic field passing through the ith winding and induces additional voltage across the winding. This magnetic field passes through the ith winding via the air and via the core resulting in the magnetic flux associated with the inductance L_{ij}^{air} and the complex inductance $\underline{\mathcal{L}}_{ij}^{\mathrm{core}}$, respectively. The latter is a complex value since the magnetic field flowing through a lossy core incurs core losses in addition to lossless magnetic energy. The lossy property of the core can be represented with a complex permeability, leading to resistive and reactive components when under the magnetic field [14], whereas the air is a lossless medium and contributes to only a reactive component. To conclude, the impedance $\underline{Z}_{ij}$ in (1) reads

$$\underline{Z}_{ij} = \underline{Z}_{ij}^{\mathrm{w}} + \mathrm{j}\omega\left(L_{ij}^{\mathrm{air}} + \underline{\mathcal{L}}_{ij}^{\mathrm{core}}\right) \tag{2}$$

[1]Some variants from Fig. 1(b) are proposed in [4], [5], and [7] by adding a capacitive element to in series or parallel with a DUT improve the accuracy of measurement.

[2]As a rule of thumb, the characteristic length of the FE discretization of a conductor should be at least three times smaller than the skin depth to accurately capture the eddy-current effect at high frequencies.

[3]The frequency is sufficiently low and the distributed capacitance effect is neglected.

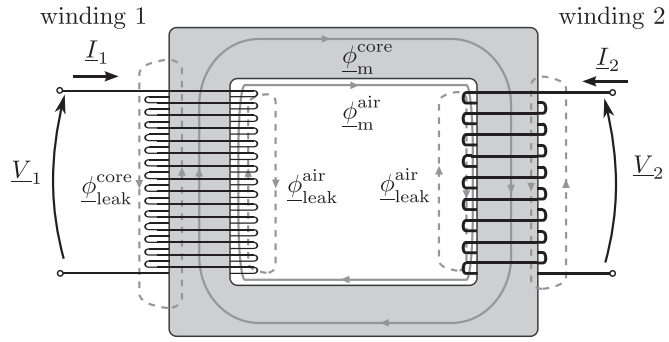

Fig. 2. Simple illustration of a two-winding device. The common fluxes in the core $\underline{\phi}_{\rm m}^{\rm core}$ and in the air $\underline{\phi}_{\rm m}^{\rm air}$ are depicted with solid lines. The leakage flux is denoted as $\underline{\phi}_{\rm leak}^{\rm core}$ if its associated magnetic field passes through the magnetic core and induces core loss, and is denoted as $\underline{\phi}_{\rm leak}^{\rm air}$ if its associated magnetic field passes through the air.

where these three terms represent the phenomenon on different medium: winding (conductor), air, and core, respectively.

To correctly model the winding resistance of a system, in addition to the conventional winding self-resistance $R_{ii}^{\rm w} = {\rm Re}\{\underline{Z}_{ii}^{\rm w}\}$, the winding mutual resistance $R_{ij}^{\rm w} = {\rm Re}\{\underline{Z}_{ij}^{\rm w}\}$ with $i \neq j$ is necessary particularly at high frequencies. The winding self-resistance represents the losses in all the windings in the system when only the net current in the ith winding is nonzero. This also includes the eddy-current losses in the other windings even when their net currents are zero (e.g., induction-heating effect). The winding mutual resistance represents the losses in all the windings in the system when only the currents in the ith and jth windings are nonzero. As previously explained, the winding loss of the system depends on the phase difference among each winding current. In other words, the winding loss of the system is

$$P_{\rm winding} = \sum_{k=1}^{n_{\rm w}} R_{kk}^{\rm w} \left|\underline{I}_k\right|^2 + \sum_{1\le i\neq j\le n_{\rm w}}^{n_{\rm w}} 2R_{ij}^{\rm w}{\rm Re}\left\{\underline{I}_i\underline{I}_j^*\right\} \quad (3)$$

where $*$ indicates the complex conjugate. Following a passive sign convention, for a given device, the winding mutual resistance $R_{ij}^{\rm w}$ can be positive or negative depending on the sign convention of voltage variables $\underline{V}_i$. If positive, the winding loss becomes highest when all the currents are in phase. For the sake of clarity, this paper follows the dot convention in Fig. 1.

B. Two-Winding Device ($n_{\rm w} = 2$) and Its T-Equivalent Circuit

In this section, we derive a detailed model and its T-equivalent circuit for a device with two windings ($n_{\rm w} = 2$) to analyze the two-winding method.

The common flux (or magnetizing flux) $\underline{\phi}_{\rm m}$, linking two windings together through a magnetic core and air (see Fig. 2), can be written based on Ampere's law as

$$\underline{\phi}_{\rm m} = \underline{\phi}_{\rm m}^{\rm core} + \underline{\phi}_{\rm m}^{\rm air} = \left(\frac{1}{\underline{\mathfrak{R}}_{\rm core}} + \frac{1}{\mathfrak{R}_{\rm air}}\right)\sum_{j=1}^{2} N_j\underline{I}_j \quad (4)$$

with N_j the number of turns of the jth winding, $\underline{\mathfrak{R}}_{\rm core}$ complex-valued reluctance of the core, and $\mathfrak{R}_{\rm air}$ the real-valued reluctance of the air. This core reluctance $\underline{\mathfrak{R}}_{\rm core}$ nonlinearly depends on the flux level in the core $\left|\underline{\phi}_{\rm core}\right|$. By decomposing the total flux into a mutual flux and a leakage flux, the corresponding impedance in (2) can be rewritten as

$$\underline{Z}_{ij} = \underline{Z}_{ij}^{\rm w} + \underline{Z}_{{\rm m},ij}^{\rm core} + \underline{Z}_{{\rm m},ij}^{\rm air} + \underline{Z}_{{\rm leak},ij} \quad (5)$$

where

$$\underline{Z}_{{\rm m},ij}^{\rm core} = {\rm j}\omega\frac{N_iN_j}{\underline{\mathfrak{R}}_{\rm core}}\ ,\ \underline{Z}_{{\rm m},ij}^{\rm air} = {\rm j}\omega\frac{N_iN_j}{\mathfrak{R}_{\rm air}} \quad (6)$$

$$\underline{Z}_{{\rm leak},ij} = \left({\rm j}\omega\underline{\mathcal{L}}_{ij}^{\rm core} - \underline{Z}_{{\rm m},ij}^{\rm core}\right) + \left({\rm j}\omega L_{ij}^{\rm air} - \underline{Z}_{{\rm m},ij}^{\rm air}\right). \quad (7)$$

In addition to the winding impedance due to eddy-current in the first term in (5), the second and the third terms are associated with the mutual fluxes through the core and the air, respectively, and the last term is associated with the leakage flux.

For illustration, a two-port network in (1) with $n_{\rm w} = 2$ can be represented by a T-equivalent circuit with an ideal transformer[4] [see Fig. 3(a)], whose turns ratio is chosen to be $N_1{:}N_2$ or $N = N_2/N_1$. This T-circuit is preferred over other variants, e.g., Pi (Π)-circuits [15], because of its consistency with the ones commonly adopted in the literature on the two-winding method [4]–[7]. This helps illustrate the effect of the winding mutual resistance in the two-winding method.

With $\underline{Z}_{{\rm leak},12} = 0$ for a two-winding device, from (5), the shunt impedance in the equivalent circuit [see Fig. 3(a)] is

$$\frac{\underline{Z}_{12}}{N} = \frac{\underline{Z}_{12}^{\rm w}}{N} + \underline{Z}_{{\rm m},11}^{\rm core} + \underline{Z}_{{\rm m},11}^{\rm air} \quad (8)$$

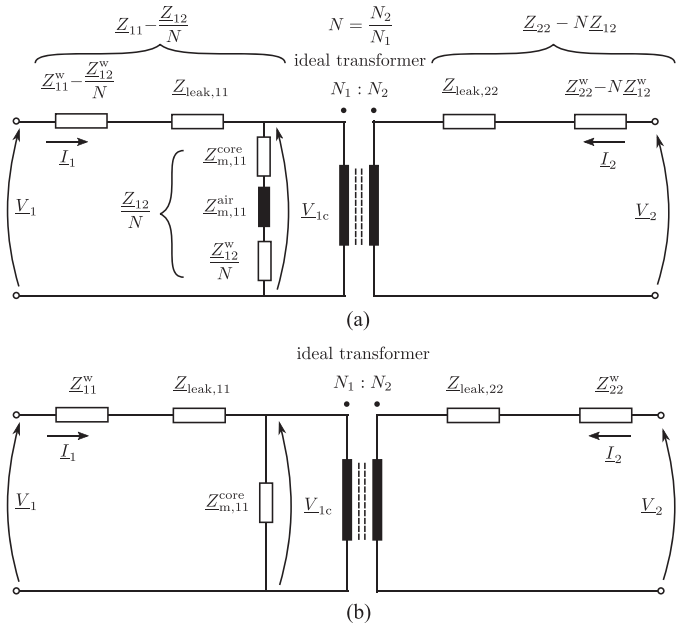

Fig. 3. T-equivalent circuit of two magnetically coupled windings with passive sign and dot conventions. (a) At high frequencies, the winding mutual impedance $\underline{Z}_{12}^{\rm w}$ appears as part of the impedance obtained from the two-winding method $\underline{Z}_{12}/N$, as well as the actual core impedance $\underline{Z}_{{\rm m},11}^{\rm core}$. The magnetizing impedance $\underline{Z}_{{\rm m},11}^{\rm core}$ and $\underline{Z}_{{\rm m},11}^{\rm air}$ arise from the common fluxes linking two windings together via the core and the air, respectively. (b) At low frequencies, the winding mutual impedance can be neglected yielding the conventional T-equivalent circuit.

[4]For two-winding systems, the turns ratio can be arbitrarily chosen [15].

whereas the other series impedances in Fig. 3(a) are

$$\underline{Z}_{11} - \underline{Z}_{12}/N = \left(\underline{Z}^{\mathrm{w}}_{11} - \frac{\underline{Z}^{\mathrm{w}}_{12}}{N}\right) + \underline{Z}_{\mathrm{leak},11} \tag{9}$$

$$\underline{Z}_{22} - N\underline{Z}_{12} = (\underline{Z}^{\mathrm{w}}_{22} - N\underline{Z}^{\mathrm{w}}_{12}) + \underline{Z}_{\mathrm{leak},22}\,. \tag{10}$$

At low frequencies, the winding mutual impedance $\underline{Z}^{\mathrm{w}}_{12}$ is negligible. Moreover, if the impedance $\underline{Z}^{\mathrm{air}}_{\mathrm{m},11}$ are omitted due to dominant common flux in high-permeability cores, the detailed equivalent circuit in Fig. 3(a) reduces to the conventional low-frequency transformer model in Fig. 3(b). Therein, the winding impedances simply become the winding self-impedance $\underline{Z}^{\mathrm{w}}_{11}$ and $\underline{Z}^{\mathrm{w}}_{22}$. The conventional magnetizing inductance and core-loss resistance seen from winding 1 correspond to the core impedance $\underline{Z}^{\mathrm{core}}_{\mathrm{m},11}$.

Note that the circuit model can be extended to include the nonlinear characteristics of the magnetic core by means of the core-impedance element $\underline{Z}^{\mathrm{core}}_{\mathrm{m}}$ as a type of saturable transformer component models [16], [17]. Even though in the linear case the T- and Pi-circuits are equivalent, in case of nonlinearity of the core, the Pi-circuit would be more suitable as more accurate [18].

III. Influence of Winding Mutual Resistance on Winding Resistance Extraction Based on Two-Winding Method

From (5), the self-resistance R_{ii} measured at the terminal of the ith winding always includes the core-loss resistance R^{c}_{ii} in addition to the desired winding resistance R^{w}_{ii} as

$$R_{ii} = \mathrm{Re}\left\{\underline{Z}_{ii}\right\} = R^{\mathrm{w}}_{ii} + R^{\mathrm{c}}_{ii} \tag{11}$$

where $R^{\mathrm{c}}_{ii} \approx \mathrm{Re}\left\{\underline{Z}^{\mathrm{core}}_{\mathrm{m},ii}\right\}$ is the equivalent core-loss series resistance [2], neglecting the core loss due to the leakage flux [$\mathrm{Re}\left\{\underline{Z}^{\mathrm{core}}_{\mathrm{m},ii}\right\} \gg \mathrm{Re}\left\{\underline{Z}_{\mathrm{leak},ii}\right\}$ in Fig 3(a)]. Hence, determining the core-loss resistance R^{c}_{ii} is necessary, which can be measured by the two-winding method. For single-winding devices (e.g., inductors), another winding is suggested to be wound, while for multiwinding devices, two windings are selected. Therefore, without loss of generality, a model of a two-winding device ($n_{\mathrm{w}} = 2$) in Section II-B is considered.

A. Two-Winding Method for Core-Loss Measurement

Fundamentally, the two-winding method [see Fig. 1(b)] excites a core with one winding and a known winding current, and measures the voltage in the other open-circuited winding [4]–[7]. With the information of the current and the voltage, the core loss[5] (or core-loss resistance) under the given excitation can be determined. Since the voltage is measured on a different winding from the excitation one, the winding loss due to the winding self-resistance of the excitation winding is excluded. Instead, as explained hereafter in this section, the measurement includes the effect of the winding mutual resistance between the two windings.

[5]If the nonlinear core loss is of interest rather than the linear lumped resistance model when the core suffers from large excitation, it is computed from the time integration of the voltage and the current [6].

Considering the circuit in Fig. 3(a) with winding 1 as the winding of interest to measure its winding self-resistance, the two-winding method is employed using winding 2 as the sensing winding to compensate the core loss. The voltage across the shunt element $\underline{V}_{1\mathrm{c}}$ [see Fig. 3(a)] can be known from the voltage measured across the open-circuit sensing winding $\underline{V}_2$ and the given turns ratio $N = N_2/N_1$, which is

$$\underline{V}_{1\mathrm{c}} = \left.\frac{\underline{V}_2}{N}\right|_{\underline{I}_2 = 0}. \tag{12}$$

Concurrently, the exciting current $\underline{I}_1$ is known from the excitation winding, and the core-loss resistance can be computed. Equivalently, this results in the shunt impedance $\underline{Z}_{12}/N$ [see Fig. 3(a)]. This results in the estimated core-loss resistance of

$$\widetilde{R}^{\mathrm{c}}_{11} = \mathrm{Re}\left\{\left.\frac{\underline{V}_{1\mathrm{c}}}{\underline{I}_1}\right|_{\underline{I}_2 = 0}\right\} = \mathrm{Re}\left\{\frac{\underline{Z}_{12}}{N}\right\} = R^{\mathrm{c}}_{11} + \frac{R^{\mathrm{w}}_{12}}{N}. \tag{13}$$

Clearly, the core-loss resistance measured with the two-winding method $\widetilde{R}^{\mathrm{c}}_{11}$ includes the effect of the mutual winding resistance between the two windings R^{w}_{12} in addition to the desired actual core-loss resistance R^{c}_{11}.

B. Effect of Winding Mutual Resistance R^{w}_{12} on Extracted Winding Resistance

Substituting the estimated core-loss resistance obtained with the two-winding method from (13) in (11), the corresponding winding self-resistance can be estimated from

$$\widetilde{R}^{\mathrm{w}}_{11} = R_{11} - \widetilde{R}^{\mathrm{c}}_{11} = R^{\mathrm{w}}_{11} - R^{\mathrm{w}}_{12}/N. \tag{14}$$

In other words, from the circuit in Fig. 3(a), the compensated impedance is the series element $\underline{Z}_{11} - \underline{Z}_{12}/N$ in (9), but not the desired winding self-impedance $\underline{Z}^{\mathrm{w}}_{11}$. Evidently, the error of the estimated winding self-impedance is due to the winding mutual resistance R^{w}_{12}, which inherits from the two-winding measurement shown in (13).

If the winding mutual resistance R^{w}_{12} is negligible ($R^{\mathrm{w}}_{12} \approx 0$), which is true at low frequencies in a system of galvanically isolated windings, this conventional method results in the estimated winding resistance being consistent with the actual winding self-resistance of our interest [$\widetilde{R}^{\mathrm{w}}_{11} = R^{\mathrm{w}}_{11}$ at low frequencies, Fig. 3(b)]. However, at high frequencies, this can lead to large errors when the winding mutual resistance becomes significant and the two windings are tightly coupled.

IV. Experimental Methodology With Improved Core Loss Compensation

A. Core-Loss Resistance Compensation

As illustrated in the previous section, the measured core-loss resistance from the two-winding method always includes the effect of winding mutual resistance. Despite being irremovable, one possible way to alleviate the effect consists in applying the two-winding method on an auxiliary device with a set of windings that possesses low winding mutual resistance. As an alternative to [3] that uses the same number of turns as the original one, in this work, we propose to perform the two-winding

method on an auxiliary with an ungapped-core counterpart and a set of single-turn 1:1 windings ($N_{1,\text{aux}} = N_{2,\text{aux}} = N_{\text{aux}} = 1$) to minimize the winding mutual resistance.

If litz wires are used, it should have as few strands as possible. One may use only a single strand extracted from a litz-wire bundle (for the test in Section VI, we used a single round wire with a diameter of 0.2 mm). Furthermore, the two windings should be wound separately and far from each other. In this manner, the winding mutual resistance between the two windings can be neglected. One can try adjusting the distance between the two windings and performing the measurement to ensure that the measured resistance remains almost constant.

The core impedance in (6) seen from the ith winding can be written as a series RL $(R_{ii}^{\text{c}}, L_{ii}^{\text{c}})$ element and a parallel RL $(R_{ii}^{\text{cp}}, L_{ii}^{\text{cp}})$ element as

$$\underline{Z}_{\text{m},ii}^{\text{core}} = \text{j}\omega \frac{N_i^2}{\underline{\mathfrak{R}}_{\text{core}}} = R_{ii}^{\text{c}} + \text{j}\omega L_{ii}^{\text{c}} = \left(\frac{1}{R_{ii}^{\text{cp}}} + \frac{1}{\text{j}\omega L_{ii}^{\text{cp}}} \right)^{-1} \tag{15}$$

where

$$R_{ii}^{\text{c}} = \omega N_i^2 \frac{\text{Im}\left\{\underline{\mathfrak{R}}_{\text{core}}\right\}}{\left|\underline{\mathfrak{R}}_{\text{core}}\right|^2}, \; L_{ii}^{\text{c}} = N_i^2 \frac{\text{Re}\left\{\underline{\mathfrak{R}}_{\text{core}}\right\}}{\left|\underline{\mathfrak{R}}_{\text{core}}\right|^2} \tag{16}$$

$$R_{ii}^{\text{cp}} = \frac{\omega N_i^2}{\text{Im}\left\{\underline{\mathfrak{R}}_{\text{core}}\right\}}, \; L_{ii}^{\text{cp}} = \frac{N_i^2}{\text{Re}\left\{\underline{\mathfrak{R}}_{\text{core}}\right\}}. \tag{17}$$

To ensure the same core loss between the auxiliary and the actual DUT, we need to control the flux density inside the core of both cases to be the same. Considering the same two-winding device in Section III [see Fig. 3(a)] and assuming the two windings are wound around the limbs of the core with the same cross-sectional area, the flux density in the DUT's core during the self-impedance measurement on winding 1 can then be estimated from the flux of winding 2 as

$$\left|\underline{\phi}_{\text{core}}\right| = \left.\frac{|\underline{V}_2|}{\omega N_2}\right|_{\underline{I}_2 = 0} \tag{18}$$

or one can use the reactive components of the measured voltage to avoid the effect of the resistive components, i.e., $||\underline{V}_2| \sin\theta_{\text{V}}|$ with θ_{V} the angle between the phasors $\underline{I}_1$ and $\underline{V}_2$, instead of $|\underline{V}_2|$. While performing the two-winding method on the auxiliary, the excitation level of its excitation winding is adjusted to yield the open-circuit voltage of the sensing winding of

$$\left|\underline{V}_{2,\text{aux}}\right| = \frac{N_{\text{aux}}}{N_2} |\underline{V}_2| \tag{19}$$

so as to regulate the flux density inside the auxiliary's core.

To measure the core resistance of the auxiliary, it is recommended to use the core with minimum airgap or without [3], [19], and [20]. This leads to lower quality (Q) factor and less errors of the measured core-loss resistance [7]. With a smaller airgap in the magnetic path, the excitation VA to generate the same level of core loss (magnetic flux) decreases, thus the power factor and the Q factor of the system also decrease [19]. In other words, the parallel $(R_{ii}^{\text{cp}}, L_{ii}^{\text{cp}})$ element representation should be considered rather than the series representation (see Fig. 4). In general, the core losses of gapped and ungapped cores are comparable at the same flux level because the airgap volume is usually smaller than the core volume, yielding $\text{Im}\{\underline{\mathfrak{R}}_{\text{core}}^{\text{gapped}}\} \approx \text{Im}\{\underline{\mathfrak{R}}_{\text{core}}^{\text{ungapped}}\}$ and thus comparable R_{ii}^{cp}. Moreover, for the same number of turns and flux level, the ungapped core yields higher L_{ii}^{cp} since $\text{Re}\{\underline{\mathfrak{R}}_{\text{core}}^{\text{gapped}}\} \gg \text{Re}\{\underline{\mathfrak{R}}_{\text{core}}^{\text{ungapped}}\}$, and thus a lower Q factor. We confirm this experimentally in Fig. 5.

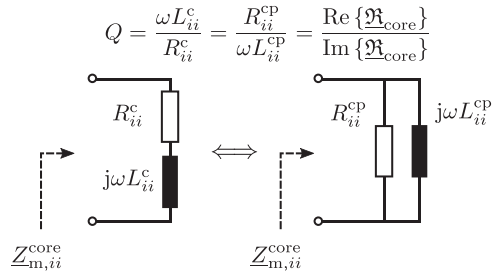

Fig. 4. Core impedance $\underline{Z}_{\text{m},ii}^{\text{core}}$ represented by a series RL element: $R_{ii}^{\text{c}} + \text{j}\omega L_{ii}^{\text{c}}$, and by a parallel RL element: $(\frac{1}{R_{ii}^{\text{cp}}} + \frac{1}{\text{j}\omega L_{ii}^{\text{cp}}})^{-1}$. Since both represent the same core impedance, the Q factor remains the same.

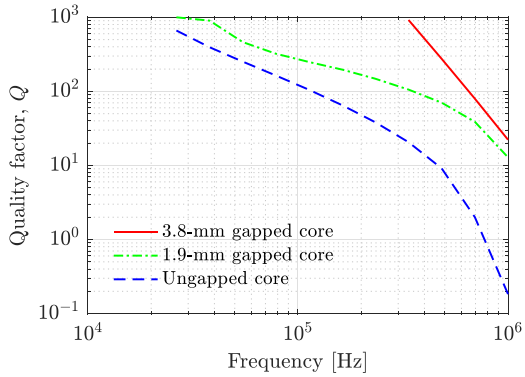

Fig. 5. Comparison of the measured Q factor of the core impedance of the auxiliary winding with gapped and ungapped cores. It is displayed only in the region where the measured resistance is positive. At low frequencies and high Q factors, the core resistance cannot be correctly measured based on the instrument accuracy.

Since the core losses of both cases are approximately the same at the same flux level $\left|\underline{\phi}_{\text{core}}\right|$, the imaginary parts of their core reluctances, $\text{Im}\left\{\underline{\mathfrak{R}}_{\text{core}}\right\}$, are comparable and, from (15) and (17), this yields

$$R_{11}^{\text{cp}} = \left(\frac{N_2}{N_{\text{aux}}} \right)^2 R_{\text{aux},11}^{\text{cp}} \tag{20}$$

where R_{11}^{cp} and $R_{\text{aux},11}^{\text{cp}}$ are the core-loss parallel resistances of the DUT and the auxiliary seen from winding 1, respectively. By converting the parallel resistance to the equivalent series resistance, the core-loss series resistance R_{11}^{c} can be found from

$$R_{11}^{\text{c}} = \frac{\left(\omega L_{11}^{\text{cp}}\right)^2}{\left(R_{11}^{\text{cp}}\right)^2 + \left(\omega L_{11}^{\text{cp}}\right)^2} R_{11}^{\text{cp}} \tag{21}$$

where L_{11}^{cp} is the measured parallel inductance of a DUT with gapped core. To avoid the effect of the resonance at high frequencies, one can use the low-frequency value because the inductance of a gapped inductor varies slightly with frequency. For an ungapped DUT, one can still use (20) without (21), but

has to replace the parallel resistance R^{cp} with the series resistance R^{c} now that the core of the DUT and the auxiliary are identical.

B. Steps of the Winding Resistance Extraction Method

The proposed procedure to extract winding resistance from impedance measurements is summarized in this section. The procedure requires the two windings of a DUT: the winding of interest and the other to measure the flux density inside the core. If a DUT is a multiwinding device, two windings are selected. If a DUT is a single-winding device, another winding should be wound with as few turns as possible and with finer strand so that it does not affect the field distribution in the winding region. In addition, the procedure requires an auxiliary device made of the ungapped-core counterpart but with a 1:1 single-turn two windings. Notably, the dot convention is followed (see Fig. 1).

We assume that the ith winding as the winding of interest and excitation winding, the jth winding as a sensing winding with $N = N_j/N_i$, and the winding self-resistance R_{ii}^{w} can be determined based on the following steps. Since, the concept is the same as the guideline in [3], the first four steps from [3] are repeated herein for completeness.

1) Measure the self-resonance frequency f_{res} ($\omega_{\mathrm{res}} = 2\pi f_{\mathrm{res}}$) of a DUT based on Fig. 1(a).[6]
2) Measure the self-impedance of the DUT, $\underline{Z}_{ii}^{\mathrm{meas}} = R_{ii}^{\mathrm{meas}} + \mathrm{j}\omega L_{ii}^{\mathrm{meas}}$, based on Fig. 1(a) together with the open-circuit voltage $\underline{V}_j$.
3) Estimate the equivalent winding distributed parallel capacitance from $C_i^{\mathrm{p}} = \dfrac{1}{(2\pi f_{\mathrm{res}})^2 L_{ii}^{\mathrm{res}}}$ where L_{ii}^{res} is the estimated inductance at the resonant frequency. L_{ii}^{res} can be estimated from the low-frequency value of the measured self-inductance L_{ii}^{meas} using a gapped core.
4) Compensate the measurement from the effect of winding capacitance, yielding R_{ii} from the formula in [3], or equivalently from
$$R_{ii} = \mathrm{Re}\left\{\underline{Z}_{ii}\right\} = \mathrm{Re}\left\{\frac{\underline{Z}_{\mathrm{C},i}\underline{Z}_{ii}^{\mathrm{meas}}}{\underline{Z}_{\mathrm{C},i} - \underline{Z}_{ii}^{\mathrm{meas}}}\right\} \tag{22}$$
where $\underline{Z}_{\mathrm{C},i} = 1/(\mathrm{j}\omega C_i^{\mathrm{p}})$.
5) (Optional for determining winding mutual resistance) Measure the small-signal core-loss series resistance of the DUT, $\widetilde{R}_{ii}^{\mathrm{c}}$, based on the two-winding measurement using winding i and winding j [see Fig. 1(b)].[6]
6) Measure the small-signal core-loss parallel resistance $R_{\mathrm{aux}}^{\mathrm{cp}}$ of an auxiliary device (ungapped transformer with 1:1 single-turn windings) based on the two-winding measurement [see Fig. 1(b)].[6] The core must be excited to have the same flux level by satisfying (19) based on the measured $\underline{V}_j$ in step 2.
7) Determine the small-signal core-loss series resistance R_{ii}^{c} from (20) and (21).

[6]The reactive power compensation by adding a capacitor to the network similar to the two-winding methods in [4], [5], and [7] can be performed instead to improve accuracy.

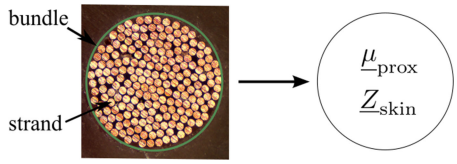

Fig. 6. Micrograph of a cross section of a real 0.1-mm-diameter 200-strand litz-wire bundle with the fill factor $\lambda = 0.4$ taken by the authors (left) being homogenized with frequency-dependent and fill-factor-dependent complex permeability and impedance (right).

8) Obtain the winding self-resistance from
$$R_{ii}^{\mathrm{w}} = R_{ii} - R_{ii}^{\mathrm{c}}. \tag{23}$$

For determining the winding mutual resistance $R_{ij}^{\mathrm{w}} = R_{ji}^{\mathrm{w}}$, the test leakage connection in Fig. 1(c) can be done. Given R_{ii}^{w} and R_{jj}^{w} from the aforementioned steps, the winding mutual resistance can be derived from (3) or Fig. 3(a) by imposing $\underline{I}_1 = -\underline{I}_2$, reading
$$R_{ij}^{\mathrm{w}} = \frac{R_{ii}^{\mathrm{w}} + R_{jj}^{\mathrm{w}} - R_{\mathrm{lkg}}}{2} \tag{24}$$
where R_{lkg} is the resistance measured from the leakage connection [3]. Notably, the compensation of core loss might still be required when measuring R_{lkg} except for a transformer with unity turn ratio because of negligible core flux. Alternatively, knowing the measured $\widetilde{R}_{ii}^{\mathrm{c}}$ and R_{ii}^{c} from steps 5 and 7, we can exploit the relation (13) and find the winding mutual resistance from
$$R_{ij}^{\mathrm{w}} = \left(\widetilde{R}_{ii}^{\mathrm{c}} - R_{ii}^{\mathrm{c}}\right) N. \tag{25}$$

V. Numerical FE Model With Homogenization of Litz-Wire Bundle

In this paper, the homogenization method in [13] and [21] is adopted to incorporate a litz-wire bundle into an FE model. To avoid high computational cost due to fine discretization of many small conductors, the litz-wire bundle is replaced by a round homogeneous conductor, in which the current density is uniform (see Fig. 6). Considering the reduced frequency X defined as the ratio of a strand radius r_{s} to a skin depth $\delta = \sqrt{2/(\sigma\omega\mu_0)}$
$$X = r_{\mathrm{s}}/\delta = \sqrt{f} \cdot r_{\mathrm{s}}\sqrt{\pi\sigma\mu_0} \tag{26}$$
with f the working frequency, σ the conductivity, and μ_0 the permeability of the conductor; its skin and proximity effects are represented by frequency-dependent complex impedance $\underline{Z}_{\mathrm{skin}}(X)$ and permeability $\underline{\mu}_{\mathrm{prox}}(X)$ (or reluctivity) as depicted in Fig. 6 [22]. They are extracted from a two-dimensional (2-D) FE cell problem. Notably, the packing type of litz-wire strands inside a bundle does not significantly affect the complex permeability [23], [24], only the fill factor does, which is defined as the ratio of a conductor area to a bundle area. Therefore, we consider the hexagonal packing in this work.

Herein, we assume that the litz wire is properly constructed yielding equal current in each strand. Twisting of strands does not significantly affect the complex permeability $\underline{\mu}_{\mathrm{prox}}$ when $X < 1$, which normally holds in practice for litz-wire

TABLE I
TRANSFORMER UNDER TEST FOR WINDING RESISTANCE EXTRACTION

Windings	
Number of turns	13:13 (full bobbin length)
Number of layers in each winding	1
Radial distance between two windings	0.34 mm
No. of litz-wire strands × strand diameter	100 × 0.2 mm
litz-wire fill factor λ	0.69
Core	
Geometry	PM 74/59
Gap	Gapped 3.80 mm, Centrepost
Material	TDK N27
Self-resonance frequency f_{res}	2.2 MHz

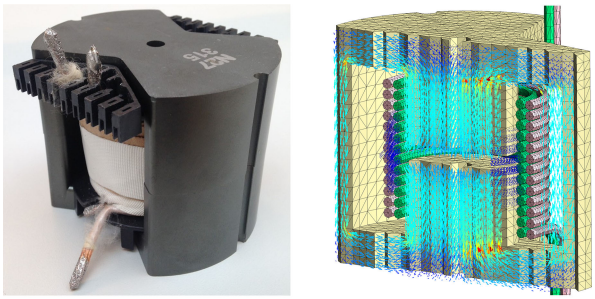

(a) (b)

Fig. 7. DUT and cut of its homogenized FE model. The distribution of the flux density is also depicted. (a) DUT. (b) Cut 3-D FE model with flux density.

applications [25]. However, the twisting imperfection can cause the circulation current and bundle-level skin effect leading to additional losses [10], [26], [27].

The homogenization-based FE computation is implemented based on the magnetic-vector-potential formulation. The proximity-effect complex permeability $\underline{\mu}_{\mathrm{prox}}$ is included directly as a property of the winding, whereas the skin-effect complex impedance $\underline{Z}_{\mathrm{skin}}$ is straightforwardly included in the electrical circuit that supplies the device. In this work, they are obtained from the 2-D FE cell problem or alternatively from [24], [28]–[30].

VI. MEASUREMENT AND NUMERICAL RESULTS

A gapped litz-wire transformer with the configuration in Table I was selected as a test case [see Fig. 7(a)]. In spite of the intended operating frequency of the core material at 500 kHz($X = 1.13$), the measurement is extended to 1 MHz($X = 1.6$) to show the effectiveness of the core loss compensation. The impedance analyzer PSM3750 NumetriQ IAI2 [31] was used for impedance measurement.

A corresponding 3-D FE magnetodynamic model was constructed as a benchmark [see Fig. 7(b)] with the open-source FE software bundle ONELAB [32] integrating the mesh generator Gmsh [33] and the FE solver GetDP [34]. The core loss was numerically modeled using the complex permeability from the

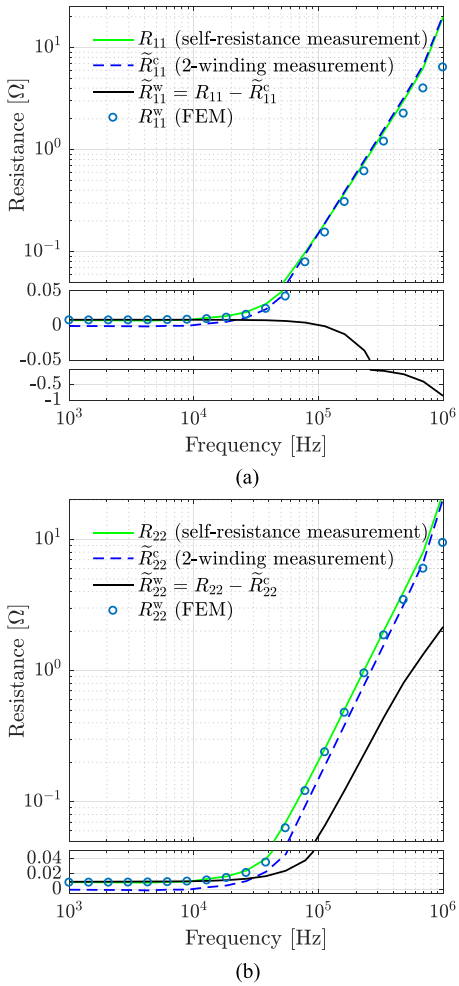

Fig. 8. Extracted winding self-resistance $\widetilde{R}^{\mathrm{w}}_{ii}$ from the measured self-resistance R_{ii} [see Fig. 1(a)] compensated by the core-loss resistance $\widetilde{R}^{\mathrm{c}}_{ii}$ obtained from the conventional two-winding method on the DUT itself [see Fig. 1(b)]. The 3-D FE results are also included for comparison. The extracted winding self-resistances show large error due to the winding mutual resistance. (a) Winding 1 (primary winding). (b) Winding 2 (secondary winding).

datasheet.[7] The litz-wire windings have been modeled with the homogenization method described in the previous section.

A. Measurement Based on Windings With High Winding Mutual Resistance

In this section, we illustrate the winding resistance extracted without careful consideration of winding mutual resistance. Since the two windings of the DUT are made of identical litz wire and have the same number of turns, the two-winding method was directly applied on the DUT.

According to Fig. 8, the primary- and secondary-winding self-resistance, $\widetilde{R}^{\mathrm{w}}_{11}$ and $\widetilde{R}^{\mathrm{w}}_{22}$, compensated for the core loss

[7] According to [3], the use of small-signal complex permeability of a core given in the datasheet can incorrectly predict small-signal core loss. However, from our numerical observations, the associated field distribution in the winding area slightly changes and does not significantly affect the winding loss. In other words, the predicted winding resistance still remains comparable despite using real permeability.

resistance do not correspond with the results from the FE computation. Besides, the estimated self-resistance of the primary winding $\widetilde{R}^{\mathrm{w}}_{11} = R_{11} - \widetilde{R}^{\mathrm{c}}_{11}$ becomes negative after the compensation, which is not physically meaningful [see Fig. 8(a)]. This occurs because the core-loss resistance measured from the two-winding measurement $\widetilde{R}^{\mathrm{c}}_{11}$ is comparable to the self-resistance R_{11}. Clearly, this shows the flaw in the measurement procedure. Despite being positive, the estimated secondary-winding self-resistance $\widetilde{R}^{\mathrm{w}}_{22} = R_{22} - \widetilde{R}^{\mathrm{c}}_{22}$ significantly deviates from the reference FE results [see Fig. 8(b)]. This error is difficult to notice in practice, leading to an underestimation of the winding resistance. Consequently, the mutual resistance from (24), $\widetilde{R}^{\mathrm{w}}_{12}$, is also erroneous due to the incorrect winding self-resistance $\widetilde{R}^{\mathrm{w}}_{11}$ and $\widetilde{R}^{\mathrm{w}}_{22}$.

Furthermore, the FE results are in good agreement with the self-resistance R_{11}, R_{22} below 300 kHz due to negligible core loss. This indicates that, at high frequencies, the core loss cannot be neglected even for small-signal excitation, and thus the proper compensation is required.

B. Improved Measurement Based on a 1:1 Auxiliary Transformer With Single-Turn Windings

According to Fig. 9, the measurement and the FE results are in good agreement in the whole considered frequency range up to 1 MHz in contrast to Fig. 8. Clearly, the core-loss resistance obtained from applying the two-winding measurement directly on the DUT, $\widetilde{R}^{\mathrm{c}}_{ii}$, is erroneous. The core-loss resistance obtained from the scaling of the results from the 1:1 auxiliary transformer with single-turn windings R^{c}_{ii} is more accurate. It starts to contribute to higher than 10% of the total resistance above 100 kHz, which is still within the recommended operating range of the core material. It becomes higher than the winding self-resistance at 1 MHz. The core-loss resistance computed from the FE model based on the complex permeability from the datasheet greatly underestimates the actual core-loss resistance. Still, the computed winding resistances remain correct.

In Fig. 9(c), the winding mutual resistance extracted based on (24), R^{w}_{12}, is displayed only above 10 kHz due to the limited accuracy of the impedance analyzer and the use of a single-turn winding. Despite aiming to reduce winding mutual resistance, the induced voltage sensed from a single-turn winding is smaller than the recommended range of the instrument at low frequencies. Nevertheless, the results from FE indicate that it is not significant in this region and the sensed voltage becomes properly measurable at high frequencies.

Below the knee point at 500 kHz, the winding mutual resistance R^{w}_{12} is approximately proportional to f^2 reflecting the proximity effect [1], [27], and it rises to the dc value of self-resistance at 30 kHz. Due to tight coupling, the winding mutual resistance becomes higher than the primary-winding self-resistance $R^{\mathrm{w}}_{12} > R^{\mathrm{w}}_{11}$ above 100 kHz, leading to the spurious measurement in Fig. 8(a). This proves that in some cases the mutual resistance is not negligible and should be carefully considered. The sum of the secondary-winding mutual resistance and core-loss resistance is in good agreement with (25)

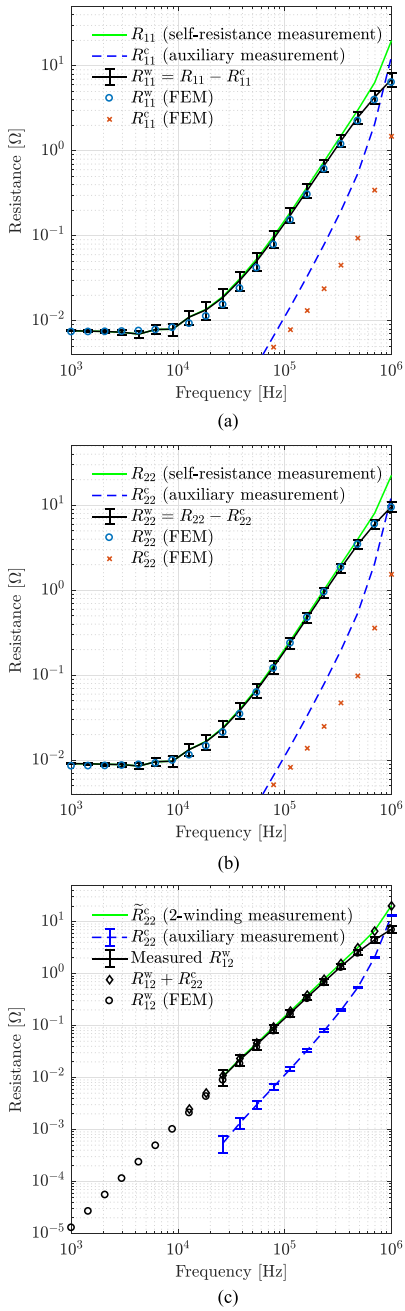

Fig. 9. Extracted winding resistances. (a) and (b) Extracted winding self-resistance R^{w}_{ii} from the measured self-resistance R_{ii} [see Fig. 1(a)] compensated by the core-loss resistance R^{c}_{ii} obtained from the 1:1 auxiliary transformer with single-turn windings. (c) Extracted winding mutual resistance R^{w}_{12}. The core-loss resistance $\widetilde{R}^{\mathrm{c}}_{22}$ measured with the conventional two-winding method is also displayed to show the effect of the winding mutual resistance or $\widetilde{R}^{\mathrm{c}}_{22} = R^{\mathrm{w}}_{12} + R^{\mathrm{c}}_{22}$. Error bars are also displayed. The 3-D FE results are included for comparison.

confirming the relation $\widetilde{R}^{\mathrm{c}}_{22} = R^{\mathrm{w}}_{12} + R^{\mathrm{c}}_{22}$ and the proposed model in Fig. 3(a).

C. Accuracy of the Measurement

This section analyzes the error made on the obtained winding resistance propagated from the main sources of uncertainties,

i.e., the impedance analyzer and the parasitic parallel capacitance. The uncertainty propagation in this study is critical because finding the winding resistances $R_{ii}^{\mathrm{w}} = R_{ii} - R_{ii}^{\mathrm{c}}$ from (23), or R_{ij}^{w} from (24) involves a subtraction and may lead to large relative error when the core loss dominates.

The impedance analyzer obtains the resistance R from: 1) $\underline{V}$, the measured voltage across a DUT; 2) $\underline{I} = \underline{V}_{\mathrm{shunt}}/R_{\mathrm{shunt}}$, the current through a built-in shunt resistor; and 3) θ the phase difference between $\underline{V}$ and $\underline{V}_{\mathrm{shunt}}$. It reads

$$R = \frac{|\underline{V}|}{|\underline{V}_{\mathrm{shunt}}|} R_{\mathrm{shunt}} \cos\theta. \tag{27}$$

Assuming the uncertainties of all the measured quantities random and independent from one another. The relative uncertainty of the resistance measured with the impedance analyzer is [35]

$$\frac{\Delta R}{R} = \sqrt{\left|\frac{\Delta\,|\underline{V}|}{|\underline{V}|}\right|^2 + \left|\frac{\Delta\,|\underline{V}_{\mathrm{shunt}}|}{|\underline{V}_{\mathrm{shunt}}|}\right|^2 + \left|\frac{\Delta R_{\mathrm{shunt}}}{R_{\mathrm{shunt}}}\right|^2 + (\tan\theta\,|\Delta\theta|)^2} \tag{28}$$

where the relative uncertainties of $|\underline{V}|$, $|\underline{V}_{\mathrm{shunt}}|$, R_{shunt}, and θ due to the instrument accuracy can be found in [31]. Herein, Δ denotes the uncertainty of a quantity.

From (28), we can determine the relative uncertainty of R_{ii}^{meas} (step 2) and $R_{\mathrm{aux}}^{\mathrm{cp}}$ (step 6) in Section IV-B. Since the auxiliary device has only a set of 1:1 single-turn windings wound separately, the capacitive coupling is negligible and the compensation of the capacitive coupling can be neglected [4], [5]. By neglecting small interwinding capacitance, obtaining the self-resistance R_{ii} still requires the compensation of the equivalent parallel parasitic capacitance C_i^{p} (step 4), which is determined from the measured self-resonance angular frequency ω_{res} (step 1) and the estimated inductance at the resonance frequency L_{ii}^{res}. The uncertainties of ω_{res} and L_{ii}^{res} constitute the uncertainty of the compensation in (22).

Note that the error on L_{ii}^{res} is a systematic error as L_{ii}^{res} is estimated from FE method. This type of error cannot be reduced with repeated measurements. In this case, we can either separate this uncertainty from the rest or combine it with the rest in quadrature [35]. The latter is adopted herein.

Assuming the uncertainties of all variables of interest random and independent from one another, we can show that the relative uncertainty of the measured self-resistance R_{ii} and the measured core-loss series resistance R_{ii}^{c} at angular frequency ω are

$$\frac{\Delta R_{ii}}{R_{ii}} = \sqrt{\lambda_1^2 \left|\frac{\Delta R_{ii}^{\mathrm{meas}}}{R_{ii}^{\mathrm{meas}}}\right|^2 + \lambda_2^2 \left(\left|\frac{\Delta L_{ii}^{\mathrm{res}}}{L_{ii}^{\mathrm{res}}}\right|^2 + 4\left|\frac{\Delta\omega_{\mathrm{res}}}{\omega_{\mathrm{res}}}\right|^2\right)} \tag{29}$$

$$\frac{\Delta R_{ii}^{\mathrm{c}}}{R_{ii}^{\mathrm{c}}} = \sqrt{\lambda_3^2 \left|\frac{\Delta R_{ii}^{\mathrm{cp}}}{R_{ii}^{\mathrm{cp}}}\right|^2 + \lambda_4^2 \left|\frac{\Delta L_{ii}^{\mathrm{cp}}}{L_{ii}^{\mathrm{cp}}}\right|^2} \tag{30}$$

where

$$\lambda_1 = \frac{1}{\sqrt{1-\alpha^2}},\ \lambda_3 = \frac{1-\gamma^2}{1+\gamma^2},\ \lambda_4 = \frac{2\gamma^2}{1+\gamma^2}$$

$$\lambda_2 = \left|\lambda_1 - 1 + 2\beta\omega^3 R_{ii}^{\mathrm{meas}} L_{ii}^{\mathrm{meas}} (C_i^{\mathrm{p}})^2\right|$$

$$\alpha = 2\omega R_{ii}^{\mathrm{meas}} C_i^{\mathrm{p}} \left(\omega^2 L_{ii}^{\mathrm{meas}} C_i^{\mathrm{p}} - 1\right)$$

$$\beta = \frac{1+\sqrt{1-\alpha^2}}{\alpha\sqrt{1-\alpha^2}},\ \gamma = \frac{R_{ii}^{\mathrm{cp}}}{\omega L_{ii}^{\mathrm{cp}}}.$$

Moreover, using the approximations similar to the studies in [4] and [5] ($R_{ii}^{\mathrm{meas}}, \omega L_{ii}^{\mathrm{meas}} \ll \frac{1}{\omega C_i^{\mathrm{p}}}$), we obtain

$$\lambda_1 \approx 1,\ \lambda_2 = 2\frac{L_{ii}^{\mathrm{meas}}}{L_{\mathrm{res}}}\left(\frac{\omega}{\omega_{\mathrm{res}}}\right)^2,\ \lambda_3 = -1,\ \lambda_4 = 2.$$

In this work, the uncertainties of ω_{res} and L_{res} are 3% and 1%, respectively. Finally, the uncertainties or errors on the obtained winding self- and mutual resistance are given by

$$\Delta R_{ii}^{\mathrm{w}} = \sqrt{(\Delta R_{ii})^2 + (\Delta R_{ii}^{\mathrm{c}})^2} \tag{31}$$

$$\Delta R_{ij}^{\mathrm{w}} = \frac{\sqrt{(\Delta R_{ii}^{\mathrm{w}})^2 + (\Delta R R_{jj}^{\mathrm{w}})^2 + (\Delta R_{\mathrm{lkg}})^2}}{2}. \tag{32}$$

According to Fig. 9, above 200 kHz where the winding self- and mutual-resistances are of the same order of magnitude, the derived errors of R_{11}^{w}, R_{22}^{w}, and R_{12}^{w} are below $\pm 15\%$, $\pm 12\%$, and $\pm 10\%$, respectively. In the same range of frequencies, these final relative errors are higher than the errors of the quantities used to obtain the winding resistances from (23) and (24) due to the subtraction processes: (R_{11} ($\pm 9\%$), R_{22} ($\pm 9\%$), R_{11}^{c} ($\pm 4\%$), R_{22}^{c} ($\pm 4\%$), and R_{lkg} ($\pm 4\%$)). Therefore, one should carefully reduce the uncertainties involved in measuring those quantities to achieve higher accuracies of extracted winding resistances. These errors mainly stem from high Q factors and small obtained resistance values, particularly significant at low frequencies. For example, the maximum relative errors of R_{11}^{w}, R_{22}^{w}, and R_{12}^{w} ($\pm 26\%$, $\pm 21\%$ and $\pm 33\%$, respectively) occur in the vicinity of 20–60 kHz ($Q > 350$) [36]. This can be alleviated by adding series capacitors during the measurement to reduce the Q factor [4], [5].

VII. Conclusion

This paper has rigorously illustrated the effect of the winding mutual resistance on the well-known two-winding method for measuring core loss and on the corresponding extracted winding resistance. Furthermore, it has demonstrated a method to mitigating this issue. The effect of the winding mutual resistance can contribute to large error in the extracted winding resistance, especially at high frequencies and with tightly coupled windings. For positive winding mutual resistance, the extracted winding resistance can underestimate the actual winding resistance of a DUT.

The guideline on the compensation of core loss has been exemplified. It consists in measuring the core-loss parallel resistance of a 1:1 auxiliary transformer with single-turn windings

excited at the same flux level, from which the actual core-loss resistance then can be obtained by scaling. The analysis has been demonstrated using a gapped litz-wire transformer with PM74 core.

As a benchmark, the 3-D FE model has been developed with an accurate homogenization method to avoid a large number of unknowns. The skin and proximity effects of a litz-wire bundle are modeled with the frequency-dependent skin-effect complex impedance and proximity-effect permeability (reluctivity). Subsequently, this paper has shown that the core-loss compensation with the conventional two-winding method must be carefully performed considering the effect of winding mutual resistance, otherwise the result can become spurious. Based on the improved compensation, the experimental and FE results are in good agreement up to 1 MHz.

REFERENCES

[1] J. H. Spreen, "Electrical terminal representation of conductor loss in transformers," *IEEE Trans. Power Electron.*, vol. 5, no. 4, pp. 424–429, Oct. 1990.

[2] M. K. Kazimierczuk, G. Sancineto, G. Grandi, U. Reggiani, and A. Massarini, "High-frequency small-signal model of ferrite core inductors," *IEEE Trans. Magn.*, vol. 35, no. 5, pp. 4185–4191, Sep. 1999.

[3] B. X. Foo, A. L. F. Stein, and C. R. Sullivan, "A step-by-step guide to extracting winding resistance from an impedance measurement," in *Proc. IEEE Appl. Power Electron. Conf. Expo.*, Mar. 2017, pp. 861–867.

[4] D. Hou, M. Mu, F. C. Lee, and Q. Li, "New high frequency core loss measurement method with partial cancellation concept," *IEEE Trans. Power Electron.*, vol. 32, no. 4, pp. 746–751, Apr. 2017.

[5] M. Mu, Q. Li, D. J. Gilham, F. C. Lee, and K. D. T. Ngo, "New core loss measurement method for high-frequency magnetic materials," *IEEE Trans. Power Electron.*, vol. 29, no. 8, pp. 4374–4381, Aug. 2014.

[6] A. Van Den Bossche and V. C. Valchev, *Inductors and Transformers for Power Electronics*. Boca Raton, FL, USA: CRC Press, 2005.

[7] F. D. Tan, J. L. Vollin, and S. M. Cuk, "Practical approach for magnetic core-loss characterization," *IEEE Trans. Power Electron.*, vol. 10, no. 2, pp. 124–130, Mar. 1995.

[8] K. Niyomsatian, J. Van Den Keybus, R. Sabariego, and J. Gyselinck, "Frequency-domain homogenization for litz-wire bundles in finite element calculations," in *Proc. ECCE Eur. 18th Eur. Conf. Power Electron. Appl.*, 2016, pp. 1–10.

[9] A. Rosskopf, E. Bar, C. Joffe, and C. Bonse, "Calculation of power losses in litz wire systems by coupling FEM and PEEC method," *IEEE Trans. Power Electron.*, vol. 31, no. 9, pp. 6442–6449, Sep. 2016.

[10] R. Y. Zhang, J. K. White, J. G. Kassakian, and C. R. Sullivan, "Realistic litz wire characterization using fast numerical simulations," in *Proc. IEEE Appl. Power Electron. Conf. Expo.*, 2014, pp. 738–745.

[11] D. R. Zimmanck and C. R. Sullivan, "Efficient calculation of winding-loss resistance matrices for magnetic components," in *Proc. IEEE 12th Work. Control Model. Power Electron.*, 2010, pp. 1–5.

[12] C. R. Sullivan, "Computationally efficient winding loss calculation with multiple windings, arbitrary waveforms, and two-dimensional or three-dimensional field geometry," *IEEE Trans. Power Electron.*, vol. 16, no. 1, pp. 142–150, Jan. 2001.

[13] K. Niyomsatian, J. Van den Keybus, R. V. Sabariego, and J. Gyselinck, "Frequency-domain homogenization for impedance characterization of litz-wire transformers in 2-D finite element models," in *Proc. 11th Int. Conf. Ecol. Veh. Renew. Energies*, Apr. 2016, pp. 1–7.

[14] D. M. Bohu, "Complex inductance and its computer modelling," *J. Electr. Eng.*, vol. 53, no. 1, pp. 24–29, 2002.

[15] R. W. Erickson and D. Maksimovic, "Multiple-winding magnetics model having directly measurable parameters," in *Proc. PESC Rec.—IEEE Annu. Power Electron. Spec. Conf.*, 1998, vol. 2, pp. 1472–1478.

[16] C. R. Sullivan and A. Muetze, "Simulation model of common-mode chokes for high-power applications," *IEEE Trans. Ind. Appl.*, vol. 46, no. 2, pp. 884–891, Mar./Apr. 2010.

[17] J. Martinez and B. Mork, "Transformer modeling for low-and mid-frequency transients-A review," *IEEE Trans. Power Del.*, vol. 20, no. 2, pp. 1625–1632, Apr. 2005.

[18] F. D. León, S. Member, A. Farazmand, P. Joseph, and S. Member, "Comparing the T and Pi equivalent circuits for the calculation of transformer inrush currents," *IEEE Trans. Power Del.*, vol. 27, no. 4, pp. 2390–2398, Oct. 2012.

[19] C. A. Baguley, B. Carsten, and U. K. Madawala, "An investigation into the impact of DC bias conditions on ferrite core losses," *Proc. 33rd Annu. Conf. IEEE Ind. Electron. Soc.*, 2007, pp. 1408–1413.

[20] V. Thottuvelil, T. Wilson, and H. Owen, "High-frequency measurement techniques for magnetic cores," *IEEE Trans. Power Electron.*, vol. 5, no. 1, pp. 41–53, Jan. 1990.

[21] J. Gyselinck and P. Dular, "Frequency-domain homogenization of bundles of wires in 2-D magnetodynamic FE calculations," *IEEE Trans. Magn.*, vol. 41, no. 5, pp. 1416–1419, May 2005.

[22] G. Meunier, V. Charmoille, C. Guérin, P. Labie, and Y. Maréchal, "Homogenization for periodical electromagnetic structure: Which formulation?" *IEEE Trans. Magn.*, vol. 46, no. 8, pp. 3409–3412, Aug. 2010.

[23] J. Gyselinck, P. Dular, C. Geuzaine, and R. V. Sabariego, "Direct inclusion of proximity-effect losses in two-dimensional time-domain finite-element simulation of electrical machines," in *Proc. 8th Int. Symp. Electr. Magn. Fields*, 2009, pp. 4–5.

[24] X. Nan and C. R. Sullivan, "An equivalent complex permeability model for litz-wire windings," *IEEE Trans. Ind. Appl.*, vol. 45, no. 2, pp. 854–860, Mar./Apr. 2009.

[25] S. Hiruma, Y. Otomo, and H. Igarashi, "Eddy current analysis of litz wire using homogenization-based FEM in conjunction with integral equation," *IEEE Trans. Magn.*, vol. 54, no. 3, 2018, Art. no. 7001404.

[26] T. Guillod, J. Huber, F. Krismer, and J. W. Kolar, "Litz wire losses: Effects of twisting imperfections," in *Proc. IEEE 18th Work. Control Model. Power Electron.*, 2017, pp. 1–8.

[27] C. Sullivan, "Optimal choice for number of strands in a litz-wire transformer winding," *IEEE Trans. Power Electron.*, vol. 14, no. 2, pp. 283–291, Mar. 1999.

[28] H. Igarashi, "Semi-analytical approach for finite-element analysis of multi-turn coil considering skin and proximity effects," *IEEE Trans. Magn.*, vol. 53, no. 1, 2017, Art. no. 7400107.

[29] H. Rossmanith, M. Albach, J. Fischer, and A. Stadler, "Improved characterization of the magnetic properties of hexagonally packed wires," *EPE J.*, vol. 22, no. 4, pp. 5–10, 2012.

[30] D. C. Meeker, "An improved continuum skin and proximity effect model for hexagonally packed wires," *J. Comput. Appl. Math.*, vol. 236, no. 18, pp. 4635–4644, 2012.

[31] "PSM3750 - NumetriQ User Manual," 2018. [Online]. Available: https://www.newtons4th.com

[32] "Open Numerical Engineering LABoratory," 2018. [Online]. Available: http://onelab.info/

[33] C. Geuzaine and J. Remacle, "Gmsh: A 3-D finite element mesh generator with built-in pre- and post-processing facilities," *Int. J. Numer. Methods Eng.*, vol. 79, no. 11, pp. 1309–1331, Sep. 2009.

[34] P. Dular and C. Geuzaine, "GetDP reference manual: The documentation for GetDP, a general environment for the treatment of discrete problems," 2018. [Online]. Available: http://www.geuz.org/getdp/

[35] J. Taylor, *An Introduction to Error Analysis: The Study of Uncertainties in Physical Measurements*, 2nd ed. Univ. Sci. Books, CA, USA, 1997.

[36] S. Prabhakaran, and C. Sullivan, "Impedance-analyzer measurements of high-frequency power passives: Techniques for high power and low impedance," in *Proc. Conf. Rec. IEEE Ind. Appl. Conf. 37th IAS Annu. Meet.*, 2002, vol. 2, pp. 1360–1367.

Korawich Niyomsatian (S'12) received the B.Eng. and M.Eng. degrees in electrical engineering from Chulalongkorn University, Bangkok, Thailand, in 2011 and 2013, respectively. He is currently working toward the double Ph.D. degrees in electrical engineering with the Université Libre de Bruxelles, Bruxelles, Belgium, and KU Leuven, Leuven, Belgium.

His research interests include design of magnetic devices with numerical methods, control of grid connected converter with high-order output filters, and new topologies of power converters.

Johan J. C. Gyselinck (M'05) received the M.Sc. and Ph.D. degree in electromechanical engineering from Ghent University, Ghent, Belgium, in 1991 and 2000, respectively.

From 2000 till 2004, he was a Postdoctoral Researcher and Lecturer with the University of Liège, Liège, Belgium. Since 2004, he has been a Professor with the Université Libre de Bruxelles, Bruxelles, Belgium. He is (co-)author of some 270 journal and conference papers. His main research interests include low-frequency numerical magnetics, electrical machines and drives, and renewables (wind and photovoltaics).

Ruth V. Sabariego received the Graduate degree in telecommunication engineering from the University of Vigo, Vigo, Spain, in 1998. She received the Ph.D. degree in applied sciences from the University of Liège, Liège, Belgium, in 2004.

She is currently an Associate Professor with EnergyVille, Department of Electrical Engineering, KU Leuven, Leuven, Belgium. She was a Postdoctoral Researcher from October 2000 till September 2013. She is (co-)author of some 230 journal and conference papers. Her research interests include applied mathematics and computational electromagnetics with a current focus on multiphysics and multiscale modeling.